Dynamics of Collapse of Flexible Polyelectrolytes in Poor Solvents

Namkyung Lee*,†,‡ and D. Thirumalai*,†

Institute for Physical Science and Technology, University of Maryland, College Park, Maryland 20742; and Max-Planck-Institut für Polymerforschung, Postfach 4138, D-55021 Mainz, Germany

ABSTRACT: The collapse kinetics of strongly charged polyelectrolytes in poor solvents is investigated by Langevin simulations and scaling arguments. We investigate the role of valence z of counterions, solvent quality, and shape of counterions on the dynamics of collapse. On the basis of the simulations, a number of results are obtained. (1) The rate of collapse, which is measured using the time dependence of the radius of gyration of the chain, increases sharply as z increases from 1 to 4. The collapse is particularly slow for the monovalent case and is observed only when the solvent quality is sufficiently poor. (2) Although the routes to collapse depend on z and the solvent quality a general collapse mechanism emerges. Upon quenching to low temperatures, counterions condense rapidly on a diffusion-limited time scale. At intermediate times metastable pearl-necklace structures form. The clusters merge at longer times with the largest one growing at the expense of smaller ones which is reminiscent of the Lifshitz−Slyozov growth mechanism. (3) The structure of the globule is controlled by z and the solvent quality. The *combined system* of the collapsed chain and the condensed counterions forms a Wigner crystal when the solvent quality is not too poor provided $z \geq 2$. For very poor solvents the morphology of the collapsed structure resembles a Wigner glass. These results are used to obtain a valence dependent diagram of states for strongly charged polyelectrolytes in poor solvents. (4) For a fixed z and quality of the solvent, the efficiency of collapse decreases dramatically as the size of the counterion increases. The shape of the counterions also affects the collapse dynamics. Spherical counterions are more efficient condensing agents than an isovalent cigar-shaped counterions.

1. Introduction

Many biological macromolecules and synthetic polymers are highly charged, thus making the study of polyelectrolytes important. Cellular processes often take advantage of shape fluctuations in charged biomolecules in performing biological functions (transcription, protein recognition, translocation of proteins across membranes, etc.). One such example of functional importance involving the behavior of an isolated biomolecule is the spectacular phenomenon of reversible condensation of DNA into toroidal structures in the presence of multivalent cations.[1] The volume decreases by nearly 4 orders of magnitude (or greater) upon collapse to a globular state. One of the key factors affecting DNA condensation is the fluctuations in the counterions which lead to an effective attractive interaction between the segments of the polyanion chain.[2−4] It is known from experiments that counterions with trivalent (or greater) valence are often required to induce chain collapse.[5,6] Another set of experiments which emphasize the importance of valence of counterions involves reversible precipitation of highly charged polyelectrolyte (PE) in aqueous solutions.[7] Precipitation requiring contraction of highly charged flexible polyelectrolyte chain occurs in solution of polystyrenesulfonate, PSS^-, only when counterions with valence 3 or 4 are added.[8,9]

In both examples, the collapse of the chain is possible because of short-range attraction between the monomers that are induced by a number of factors including the condensation of counterions. The mechanism of condensation of DNA is dictated by an interplay of several effects such as bending rigidity,[10,11] valence and size of counterions,[12] and hydration forces. Because intrinsic stiffness is not relevant for flexible PE, it might seem that the collapse transition is simpler in this instance than in stiff PE. However, because of the interplay between the bare electrostatic interactions, counterion condensation, and the solvent quality, even the (expected) phase diagram of highly charged flexible PEs is quite complicated. Simulations[13−15] and scaling arguments[16−18] are beginning to provide a picture of the possible structures that emerge in highly charged polyelectrolytes in which correlations induced by counterions play a crucial role.[13−15,18−22] In fact, all the relevant transitions are driven by condensation (Manning) of counterions.[23]

Synthetic and natural macromolecules usually contain hydrophobic moieties (for which water is a poor solvent), which makes it necessary to consider PE chains under poor solvent conditions. Because correlations between counterions are important in describing the shape of PE chains in poor solvents an analytical description is difficult. Although there have been some earlier attempts to understand the structure of charged macromolecules,[24] only recently have systematic investigations begun. Most attention has focused on the equilibrium conformations of weakly charged polyelectrolytes in poor solvents in the presence of monovalent cations. The solvent quality is measured with respect to the neutral polymer. The earliest treatment of the conformation of a polyelectrolyte chain in poor solvents is due to Khokhlov.[24] He showed, by balancing the electrostatic contribution and the surface tension contribution to the free energy, that a weakly charged PE would adopt a cylindrical shape. It has been subsequently appreciated that such a conformation is unstable to capillary fluctuations which causes the chain to split into clusters ("pearls") connected by stretched strings. Although such pearl-necklace structures were proposed in other contexts they were argued to be equilibrium structures for weakly charged PE in poor solvents by Dobrynin, Rubinstein, and Obukhov.[25]

† University of Maryland.
‡ Present address: Max-Planck-Institut für Polymerforschung.

10.1021/ma001604q CCC: $20.00
Published on Web 04/11/2001

Simulations of weakly charge PE chains[26] seem to confirm the existence of pearl-necklace structures predicted on the basis of Rayleigh instability.[27]

It is known that strongly charged PE in poor enough solvents can undergo coil−globule transition. Currently, no detailed understanding of the structures of the collapsed phase of strongly charged PE chains in poor solvents exist. The notable exception is the work of Micka et al.[14] who have examined the structural properties of PE chains in the presence of monovalent counterions. Despite its obvious importance, there has been no study of the dynamics of collapse of PE chains as a function of a number of possible controlling parameters. The many variables (solvent quality, valence of the counterions, and shape and size of counterions) that control collapse dynamics makes this a complicated problem. In this paper we provide a description of the dynamics of the collapse of strongly charged PE in poor solvents. We focus on the generic mechanisms of collapse of flexible PE and their dependence on the valence and size of counterions and solvent quality. We consider polyelectrolyte chains that are highly charged so that $f(l_B/b)^2 > 1$ where f (=1 is the example considered here) is the fraction of charged monomers and $l_B = e^2/4\pi\epsilon k_B T$ is the Bjerrum length, with T being the temperature and ϵ is the dielectric constant of the solvent, and b is the size of the monomers. Since the PE is highly charged all the effects described here are directly a consequence of counterion condensation. Here we discuss a number of novel results from our simulations on the collapse dynamics of strongly charged PE chains in poor solvents.

The major results of this study, which are obtained using a combination of Langevin simulations and scaling arguments, are as follows.

(a) Upon quench to poor solvent conditions from Θ-solvents (for the uncharged backbone), the highly charged PE undergoes a transition from a coil to a compact globular conformation. The kinetics depends dramatically on the valence of the counterion z. For all range of parameters the slowest kinetics is found for $z = 1$, and generally the rate of globule formation increases with z. There are no qualitative differences in the dynamics of approach to the globular state between $z = +3$ and $z = +4$.

(b) There are profound differences in the mechanisms (controlled by the valence z) of the (equilibrium) globule formation. For $z = 1$ and $l_B/b > 1$, a large fraction (>0.9) of the condensed counterions and monomers form ion pairs. The range of the resulting attractive interaction between the dipoles (arising from ion pairs) is too short, so that nucleation and propagation of locally condensed globules is slow. The initial condensation of higher valence counterions ($z \geq 2$) produces conformations that bear a striking resemblance to pearl-necklace structures. Such structures are predicted to be equilibrium states for weakly charged polyelectrolytes in poor solvents[25,26,28] (and polyampholytes[29]) based on an analogy to Rayleigh instability in charged droplets.[27] The number of globules in the necklace decreases with increasing z. Since the final (globular) conformation involves coarsening of the pearls in the necklace, we find that the collapse rate increases as z increases.

(c) The morphology of the condensed polyelectrolyte (the equilibrium structure) depends critically on the solvent quality. If the solvent is not too poor, then the conformation of the counterion and the charged polymer is a Wigner crystal. For $z \geq 2$, we find a bcc-like crystal. When the solvent quality is very poor amorphous structures (Wigner glasses) are formed. In this regime, the dynamics is very slow. On the time scales of observation the ordered structure is not reached. The boundary between the two, which is obtained using scaling arguments, is given by $|v_2|_c \approx b^{5/2} l_B^{1/2} z^{1/2}$, where v_2 is the excluded volume parameter which is negative in poor solvents.

(d) If the quality of the solvent is fixed (for a given value of $|v_2|$) then the efficiency of chain collapse depends dramatically on the size of the counterions. The rate of approach to the globular conformation increases as the size of the counterion decreases at a fixed value of z. The shape of the counterions also affects the collapse dynamics and the structure of the globule. Trivalent spherical counterions ($l = b$) are found to cause rapid collapse compared to three connected monovalent (cigar-shaped, $l = 3b$) counterions.

The rest of the paper is organized as follows: The model and simulation details are given in section II. We discuss the effects of solvent quality, valence of counterions, and their shape and structure on the collapse dynamics and on the structure of the globular phase in section III. We present a phase diagram as a function of valence in the plane of v_2 (specifying solvent quality) and l_B (measuring the electrostatic interaction). In section IV, we provide a comparison of collapse dynamics of PE chains and homopolymer collapse. A brief conclusion is given in section V.

2. Model and Simulation Technique

Model. We model the polyelectrolyte as a flexible chain consisting of N monomers each of which carries a charge of -1 (measured in units of e). The van der Waals radius of each monomer is $b/2$. Successive monomers are connected by an elastic spring with spring constant $3k_BT/b^2$. This value is large enough that we do not see significant excursions from the equilibrium bond distance, b. The valence of the cations (the counterions) varies from $z = 1 - 4$ and their number is determined by the condition of charge neutrality. The nonelectrostatic interaction between the particles (monomer or counterions) i and j with radii σ_i and σ_j respectively that are separated by r_{ij} is taken to be

$$H_{LJ}(r_{ij})/k_BT = \epsilon_{LJ}\left[\left(\frac{r_o}{r_{ij}}\right)^{12} - 2\left(\frac{r_o}{r_{ij}}\right)^{6}\right] \quad (1)$$

where average bond length $r_o = (\sigma_i + \sigma_j)$. In our model system we use the Lennard-Jones interaction parameter ϵ_{LJ} to control the quality of the solvent.The charged particles interact via the Coulomb potential

$$H_C(r_{ij})/k_BT = \frac{l_B z_i z_j}{r} \quad (2)$$

where z_i and z_j are the valence of particles i and j. Solvent quality is expressed in terms of the second virial coefficient

$$v_2 = \int_v d^3\mathbf{r}\,(1 - e^{-H_{LJ}/k_BT}) \quad (3)$$

which is negative for poor solvents. Experimental studies of polyelectrolytes are often conducted in aqueous solution. Typically PE chains contain hydrophobic moieties (aromatic groups in RNA for example) for which water is a poor solvent. We refer to the solvent as hydrophobic if v_2 is negative, and the strength of hydrophobicity depends on the value of v_2.

For simplicity, the nonelectrostatic potential between the counterions and the backbone monomer is also taken to have the standard Lennard-Jones form with the same value of ϵ_{LJ} as for the monomer−monomer interaction. We have also verified that our results are qualitatively similar if the attractive part of the Lennard-Jones interaction between the monomer and the counterion is neglected. This shows that the chain collapse described here is mediated by a balance between renormalization of the electrostatic interactions due to counterion condensation and the effective hydrophobic interaction between the monomers. A goal of this work is to explore the plausible scenarios for PE collapse for different strengths of the hydrophobic interaction.

The chain and the counterions are placed in a truncated octahedron (Wigner-Seitz cell of bcc) unit cell with the lattice constant L. The volume of the unit cell is $V = {}^1/_2L^3$. The long range nature of the Coulomb interaction is treated by accounting for interactions with the image charges in a periodically replicated system.[30] This is achieved using Ewald summation. The computations were done with $N = 120$ ($L = 40\sigma_m$) or $N = 240$ ($L = 80\sigma_m$). Most of the results presented here are for the latter case so that the monomer density $\rho_m = N/V = 9.36 \times 10^{-4}\sigma_m^{-3}$, where σ_m ($=b/2$) is the radius of the monomer.

Solvent Conditions. For sufficiently large values of ϵ_{LJ}, the effective interaction between the monomers for the uncharged polymer chains is attractive. In this situation the polymer chain will undergo a collapse transition at temperatures less than the Θ temperature. The solvent condition corresponding to large ϵ_{LJ} values will be considered "hydrophobic". For a fixed chain length N it is necessary to determine approximately the value of the Θ temperature. At $T = \Theta$ the attractive and repulsive interactions cancel each other so that the end-to-end distance $R_N^2 \sim N^{2\nu}$ with $\nu = 0.5$. To obtain the precise estimate of the Θ temperature, we use the standard scaling relation

$$\frac{R_N^{\,2}}{Nb^2} = f(\Delta T\sqrt{N}) \tag{4}$$

where $\Delta T = (\Theta - T)/\Theta$. For a fixed value of R_N^2/Nb^2, a plot of ϵ_{LJ}^{-1} vs $N^{-1/2}$ yields a straight line from which we determined that $\epsilon_{LJ,\theta^n} = 0.30 \pm 0.05$ ($v_2 = -0.06b^3$). For the finite chain size with $N = 240$ the effective Θ-temperature corresponds to $\epsilon_{LJ} = 0.5$ and $v_2 = -1.9b^3$. We find that the neural chain undergoes a coil−globule transition (homopolymer collapse) for values of $\epsilon_{LJ} \geq 1.2$. For $0.5 < \epsilon_{LJ} < 1.2$($-1.9b^3 < v_2 < -10.3b^3$) the size of the neutral chain with $N = 240$ is less than that of that found under Θ conditions but is not a compact globule. We define this regime to be weakly hydrophobic. When $\epsilon_{LJ} < 0.5$ ($v_2 < -1.9b^3$) the neutral chain is under Θ-solvent conditions. For values of $\epsilon_{LJ} > 1.2$($v_2 < -10.3b^3$), the solvent is poor enough that the equilibrium conformation of the neutral chain is a globule. The solvent condition corresponding to large $\epsilon_{LJ} > 1.2$ values will be considered "hydrophobic".

A similar way of classifying solvent conditions has been used before.[14] In the polyelectrolyte problem changing the temperature alters the electrostatic interactions even if l_B is fixed. For this reason it proves convenient to vary ϵ_{LJ} (or equivalently v_2) so that the interplay between solvent quality and electrostatic interactions can be studied.

In the presence of charges (especially under conditions when counterions condense) the effective Θ temperature can be different from the values reported above. Without presence of counterions, chains are swollen due to the repulsive interaction between the charges, which gives a positive electrostatic contribution to the persistence length. Counterion condensation increases the value of the Θ temperature from that of the neutral value. This is because there is an additional attractive interaction that arises because of softening of the electrostatic repulsion. The precise estimate of the effective Θ temperature will depend on the specific system (value of l_B, concentration of the counterions, its valence). For example, at the typical ion concentration ($\rho_m = 9.36 \times 10^{-3}\sigma_m^{-3}$ and $l_B = 5.0b$) the chain is swollen for $\epsilon_{LJ} > 1.2$ (poor solvent condition for the neutral chain) when the counterion is monovalent.

The preceding example shows that the conformation of the chain is determined by a balance between the effective hydrophobicity (parametrized in our model by ϵ_{LJ} or equivalently v_2) and electrostatic interactions mediated by counterions. For simplicity we use ϵ_{LJ} for the neutral chain to merely indicate the effective strength of the hydrophobic interactions. In what follows we systematically investigate the effects of valence and the strength of the hydrophobic interaction in determining the morphology of the collapsed structures.

Simulations. To probe the kinetics of collapse we assume that the chain dynamics is described by the Langevin equation. The equations of motion are integrated with a step size $\Delta t = 10^{-3}\tau$ where the unit of time $\tau = b^2/2D = b^2\zeta/2k_BT$, where ζ is the friction coefficient. The positions of the particles are updated using

$$R_n(t + \Delta t) = R_n(t) + \frac{1}{\zeta}F_n\Delta t + \eta(t)(\Delta t)^{1/2} \tag{5}$$

where $R_n(t)$ is the position of monomer or counterion n at time t, $F_n(t)$ is the total force on the particle n due to the other particle, and η is a Gaussian random force on particle n due to the presence of solvent. We have carried out simulations starting from various initial conditions. For each initial condition the equation of motion was integrated for relatively long times (typically for $\approx 300\tau$). To obtain results with relatively small errors averages of various quantities are taken over at least 40 independent trajectories.

Role of Initial Conditions. In most of our simulations we start from an ensemble of initial conditions which corresponds to the Θ-solvent for the neutral chain. For $N = 240$ this corresponds to $\epsilon_{LJ} \leq 0.5$ ($v_2 = -1.9b^3$) for $N = 240$. Starting from these conditions, the temperature is lowered so that counterion condensation becomes possible. This process effectively lowers the second virial coefficient so that the Θ temperature of the chain increases. For this initial conditions the radius of gyration of the chain initially increases.

We have also tried quench conditions by initially equilibrating the charged chain at temperatures where there is no counterion condensation. At such temperatures, the PE chain is stretched due to the mutual repulsion between the monomer charges. If a quench from the high temperature to a low temperature is carried out, the radius of gyration is found to monotonically decrease with time. We have verified that, after a transient time (in which the counterion condensation is complete), neither the collapse mechanism nor the morphology of the final structures depend on the initial conditions. Thus, the overall mechanisms for collapse is independent of the initial conditions. In our simulations hydrodynamic interactions are neglected. For homopolymers Pitard[31] has shown that accounting for hydrodynamic interactions using preaveraged Oseen tensor does not qualitatively alter the scenario for collapse. In this article we are interested mainly in exploring the variations in collapse mechanism in PE chains as a function of number of characteristics of the counterions. We expect that qualitative conclusions will remain valid even if hydrodynamic interactions are taken into account.

3. Results

A. Effect of Valence and Solvent Quality on Collapse Dynamics. The dynamics of collapse of the PE chain is determined by a balance between hydrophobic interactions and charge renormalized electrostatic potentials. If the electrostatic repulsion is dominant, as would be the case at intermediate temperatures, then the chain would be in an extended conformation. At low temperatures such that the Manning parameter $\xi_M = l_B/b > 1/z$, counterions condense and the chain dynamics and structure are determined by a combination of renormalized electrostatic interactions and the effective attractions between monomers due to poor

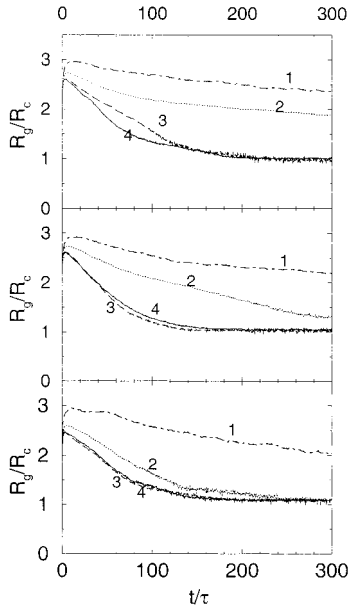

Figure 1. Dependence of $\langle R_g(t)\rangle/R_c$ for various solvent conditions. The values of v_2 are $-0.06b^3$ (Θ-solvent), $-3.7b^3$ (weakly hydrophobic), and $-25.8b^3$ (hydrophobic) for the top, middle, and bottom panels, respectively. The radius of gyration for compact globule is $R_c = 4.08b$. The numbers on the curves are the values of the valence of counterions.

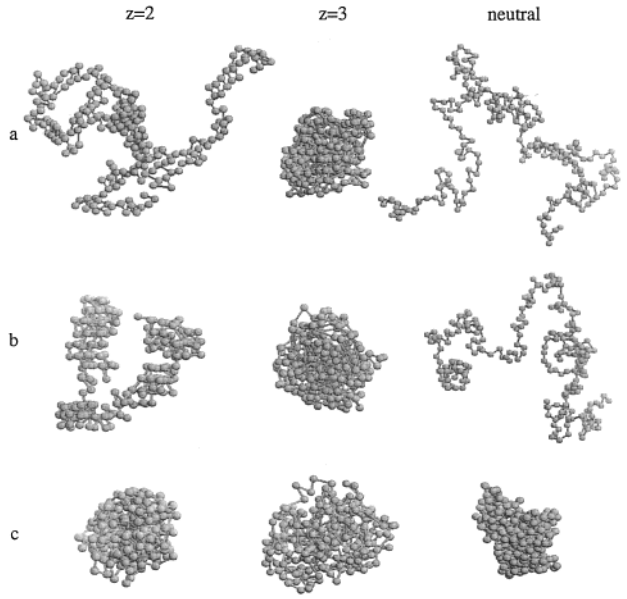

Figure 2. Snapshots of the polyelectrolyte chain at $t \approx 300\tau$ for the three solvent conditions described in Figure 1. For comparison, the conformation of the neutral chain is also given. Part a shows that only $z = 3$ induces compact globule formation. Both the neutral chain and the PE chain with $z = 2$ are extended. There is evidence for local clusters in the PE chain with $z = 2$. These effects are more pronounced for the weakly hydrophobic case shown in Part b. For the hydrophobic solvent condition, the chain is collapsed for both divalent and trivalent counterions. Although the neutral chain forms a globule the pair correlation function reveals no order as it does for the counterion-induced condensation.

solvent conditions. To determine how these effects are manifested in the kinetics of collapse we consider three solvent conditions separately.

Near Θ Solvent Condition ($v_2 < -1.9b^3$). It is known that the neutral polymer behaves as an ideal chain as long as $v_2 \leq -b^3N^{-0.5}$. In our simulations, we find that for $N = 240$, when $v_2 \leq -1.9b^3$ ($\epsilon \leq 0.5$ in eq 1), the neutral chain is ideal; i.e., the radius of gyration $R_g \sim bN^{\nu}$ ($\nu = 0.5$). Thus, in this solvent condition the collapse, if it occurs at all, can only happen because of Manning condensation that gives rise to charge-mediated attractions. We used Langevin simulations to monitor the dynamics of approach to the globular conformation. The values of $v_2 = -0.06b^3$ and $l_B = 5.0b$. The collapse kinetics is monitored using the time dependence of $\langle R_g(t)\rangle/R_c$ (Figure 1a) where R_c is the size of the compact globule, $R_c = 4.08b$. We see that on the time scale shown ($t = 300\tau$) in Figure 1a only trivalent and tetravalent counterions induce globule formation. The chain is still extended at $t \approx 300\tau$ for monovalent and divalent cations. The rate of approach to the globular conformation is larger for $z = 4$, and it decreases as z is decreased. For divalent cations, the chain collapses at $t \approx 600\tau$. We expect collapse of the PE chain to occur for large $l_B/b > 5$ for $z = 1$.

The radius of gyration increases initially in the curves displayed in Figure 1a. This is because the neutral chain is first equilibrated and then the charges are introduced with concomitant change in l_B. Thus, at very short times, there is a local expansion of the PE chain on time scales prior to the diffusion-limited time needed for counterion condensation. After this occurs, the chain begins to contract as seen in Figure 1a. If the initial conditions had been such that the equilibration had been done with charged chain and then a quench to a lower temperature been performed then $\langle R_g(t)\rangle$ would decrease monotonically with t. This is indeed the case for all the simulations. Thus, the morphology of the chain as well the dynamics of approach to the final structure is independent (apart from the time in which counterions condense) of the initial conditions.

The typical conformations of the chain for various values of z at $t \approx 300\tau$ are displayed in Figure 2. For comparison we also show the equilibrium structure of the neutral chain. These snapshots reinforce the conclusions drawn based on the decay dynamics of the chain.

Because the neutral polymer chain is ideal, it follows that collapse is mediated by counterion condensation. It is easy to show that upon counterion condensation the charge on the chain reduces from Nf ($f = 1$ in our example) to $R_g k/zl_B$ where $k \approx -\ln \phi$ with ϕ being approximately the volume fraction of the counterions. This charge renormalization alone is insufficient to describe collapse of the chain under Θ-solvent conditions. However, counterion condensation leads to an additional attraction between monomers that effectively make the solvent poor. In the case of monomers, the attraction is due to dipole−dipole interaction between bound pairs of counterion and the backbone charge (see below). Because of the counterion-mediated attraction (the nature of which depends on z) between the monomers the PE chain undergoes a coil−globule transition. Our results show that multivalent cations are more efficient in causing such a collapse.

There are two effects of counterion condensation: (i) The overall charge of the polyanion is greatly reduced. (ii) Upon counterion condensation there is an effective attractive attraction which effectively makes the solvent poor. Because collapse occurs under Θ-solvent conditions, we conclude that it is the latter effect that causes the transition to a compact globule structure. In the absence of such an induced attraction, the PE chain would be extended at intermediate and low temperatures with considerably diminished charge per mono-

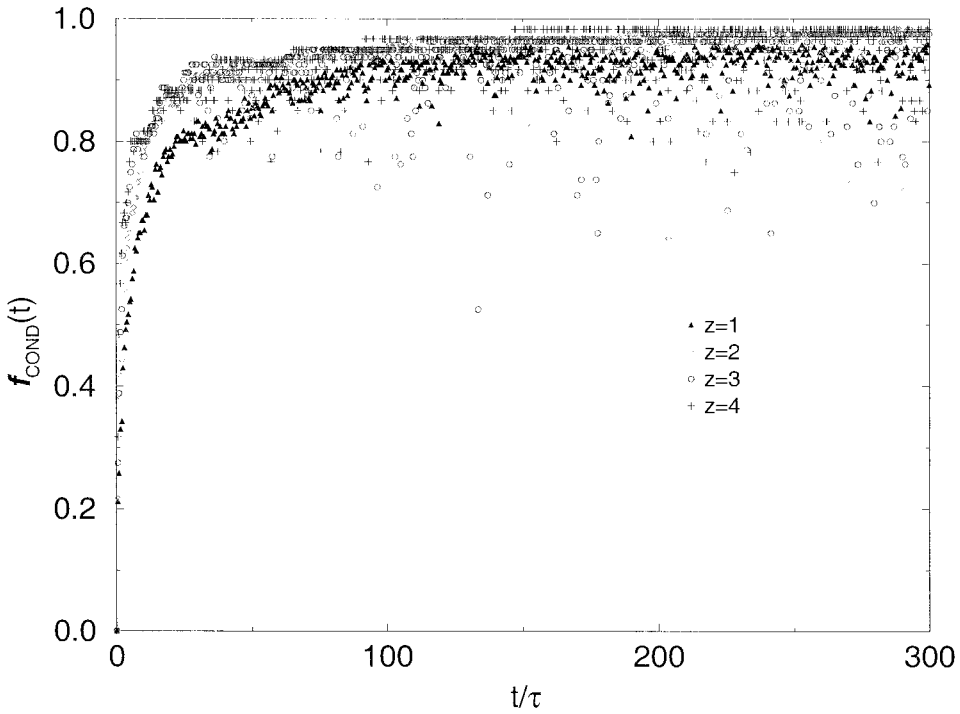

Figure 3. Fraction of condensed counterions as a function of time with $v_2 = -25.8b^3$ ($\epsilon_{LJ} = 2.0$). The time required for $f_{COND} = 0.9$ is nearly independent of z. We find that the condensation rate does depend mildly on v_2 (data not shown).

mer. The strength and nature of the induced attraction depends on z. For monovalent ions it is the dipole−dipole interaction whereas for higher values of z "ion-bridging" effects become important (see below).

Weakly Hydrophobic Conditions ($-1.9b^3 \le v_2 \le -0.3b^3$). In Figure 1b, the time dependence of $\langle R_g(t)\rangle/R_c$ is shown. Under weakly hydrophobic conditions, the globular conformation is reached for all $z \ge 2$ at time scale $t = 300\tau$. However, the approach to the globular form is slowest for $z = 2$. This is because the range over which the effective attraction comes into play is smallest for $z = 2$, and this leads to the relatively slow dynamics. Under weakly hydrophobic conditions, the neutral chain is not compact (Figure 2b). Thus, the induced attraction caused by counterion condensation, which effectively makes the solvent poorer, enables globule formation.

Hydrophobic Conditions ($v_2 \le -10.3b^3$). In this situation, the neutral chain would adopt a compact globular conformation. Thus, we expect that counterion condensation would only accelerate the rate of globule formation. This is indeed the case as can be seen in Figure 1c. With $\epsilon_{LJ} = 2.0$ and $v_2 = -25.8b^3$, even monovalent counterions enable the PE chain to reach the globular state on the time scale of our simulation. It is clear from Figure 11 that the neutral chain would not form a globule for $t \approx 300\tau$. Thus, the enhancement in the rate of globule formation is due to induced attraction resulting from counterion condensation.

Although globule formation occurs readily (especially for multivalent counterions) at low enough temperatures the structure of the "equilibrium" globule depends sensitively on the degree of hydrophobicity. A comparison of the globular state in the three cases clearly illustrates this (Figure 2).

The inability of monovalent ions in efficiently inducing chain collapse (on the time scale of simulations) has prompted us to examine the typical structures at long times. For $\epsilon_{LJ} = 0.3$ and 0.7 (the former corresponds to Θ conditions, and the latter is weakly hydrophobic) we find evidence for the formation of pearl-necklace structures. This is consistent with the observations by Micka et al.[14] who have found such structures for $N = 94$ even under more strongly hydrophobic solvent condition ($\epsilon_{LJ} = 6.0$, $l_B = 3.0b$) at concentration lower than $2 \times 10^{-3}\sigma^{-3}$. When $\epsilon_{LJ} = 2.0$, $l_B = 5.0b$, we find that in addition to pearl-necklace structures there are also partially collapsed conformations. This suggests a plausible coexistence between these typical conformations. Estimates of renormalized second virial coefficient due to dipole−dipole interaction upon counterion condensation[18] shows that even with the bare $v_2 = -0.06b^3$ ($\epsilon_{LJ} = 0.3$) the chain is effectively in a poor solvent. These observations lead us to conclude that in all likelihood the pearl-necklace structures are metastable and the

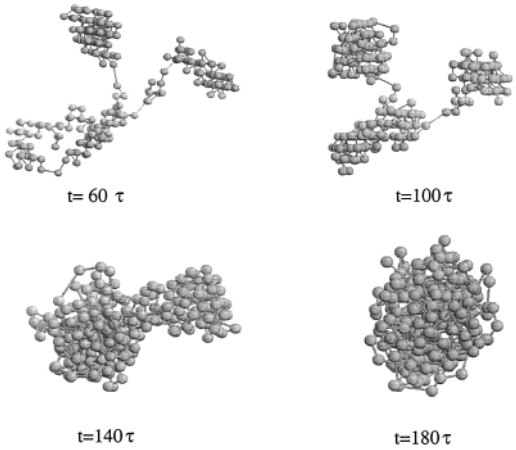

Figure 4. Sequence of snapshots in the transition from an extended conformation to a collapsed state for the PE chain with $z = 2$, $v_2 = -15.2b^3$. These snapshots pictorially confirm the mechanism for globule formation. At early times ($t \approx 60\tau$) local clusters composed of monomers form. These clusters already appear to have the order seen in the final collapsed conformation. This suggests a hierarchy of growth of the globule. At longer times, the clusters merge via a Lifshitz−Slyozov growth process until the globule is assembled.

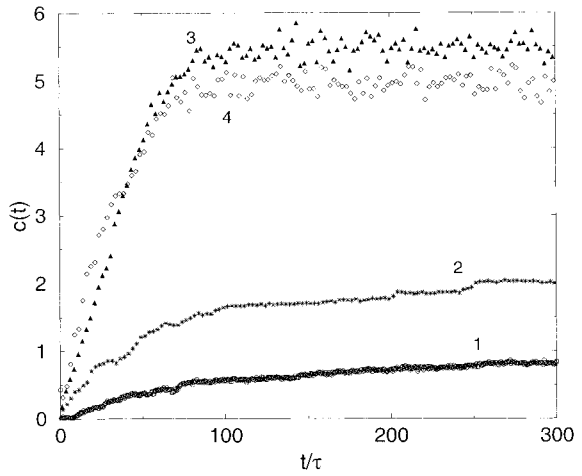

Figure 5. Time dependence of the correlation function $c(t)$ (see eq 6) probing the range of counterion-mediated contacts for various values of z. $v_2 = -0.06b^3$. Longer range contacts leading to ion-bridging develop as z increases.

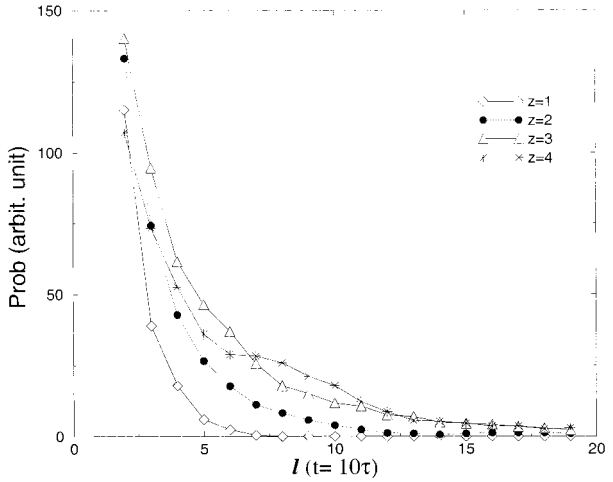

Figure 6. Probability of forming loops (ion-bridging) as a function of loop length l at $t = 10\tau$. This time is shortly after the electrostatic interaction is turned on. About 70% of counterions are condensed. This figure clearly shows that longer loops are formed with greater probability as z increases.

transition to globular state would occur at longer times at low enough temperatures and (or) at large densities.

B. Three stages of Collapse. Despite the dramatic variations in the time scale of collapse with respect to z and solvent quality the approach to the globular structure can be surmised to occur in roughly three stages. The initial stage is marked by the condensation of counterions to the strongly charged polyanion backbone. The time scale of condensation τ_{COND} is presumably controlled by diffusion process. In particular $\tau_{COND} \approx \rho_m^{-2/3}\zeta k_B T$ which for our simulation is approximately 25τ. We calculated the time required for 90% of counterions to condense. The time scales are determined only by ρ_m and are approximately *independent* of z. In Figure 3 we show the number of counterions condensed as a function of t. We see that the rate is independent of z. The condensation time scale is diffusion-limited and is determined by the density of counterions. The fraction of condensed ions does depend on l_B.

After counterion condensation, globular clusters containing both monomers and counterions form. This is most vividly illustrated in Figure 4 which shows a sequence of snapshots of the conformations of the PE chain enroute to the globular state. In the intermediate time regime $\tau_{COND} < t < \tau_{CLUST}$, one observes locally formed clusters connected by strings. By locally, we mean that the monomers in a given cluster are predominantly neighbors; i.e., they are not separated by large distances along the chain contour. At long times the clusters merge and the largest cluster grows at the expense of smaller ones. This is very reminiscent of the Lifshitz−Slyozov growth mechanism.[32] The clusters, the number of which depends on z and v_2, are connected by "strings" giving rise to a pearl-necklace structure. This process occurs in the time regime $\tau_{COND} < t < \tau_{CLUST}$. For $t \gg \tau_{CLUST}$, coarsening of the clusters takes place until the equilibrium globular structure is formed.[33] We have shown[33] using a dynamical variational theory[31] that $\tau_{COLL} \sim (l_B/b)^{-4/3}b^2/D$. Using simulations it was shown[33] that the merging of clusters occurs by the Lifshitz−Slyozov[32] growth mechanism so that $\tau_{COLL} \sim N$.

Thus, the counterion-mediated collapse of strongly charged PE in poor solvents takes place in the stages and is characterized by the time scales τ_{COND}, τ_{CLUST}, and τ_{COLL}. This general scenario is qualitatively valid under different solvent conditions. However, the structure of the globule depends very strongly on the solvent quality (see below).

In the range of parameters (the monomer density ρ_m, temperature, and solvent quality) of our simulation the pearl-necklace structures are *always* metastable. However, we suspect that the low enough densities the pearl-necklace structures may be thermodynamically stable equilibrium structures. The simulations of Micka et al.[14] show that this is the case.

C. Variations in Collapse Mechanism: Valence Dependence. Consider the monovalent case, $z = 1$. When the monovalent counterions are condensed they combine with the charges on the backbone of the polyanion to form ion pairs. Even though the condensed counterions are mobile along the polyanion backbone, we can think of the effect of counterion condensation as having generated random dipoles of magnitude $p \approx ed$ where $d \approx b$ is the distance between the monomer and the bound ion. Contacts between distinct segments of the chain can form provided the attractive energy between the dipoles must exceed $k_B T$. Thus, the range of (needed for collapse) attractive interactions $r_t \approx (l_B b^2)^{1/3} < l_B$. Since the range over which monomers condense to generate the local globules in the necklace is relatively small, we expect cluster formation to occur only on short length scales. This generates a relatively large number of clusters, and their subsequent merger (nucleation) to form a fully compact globule is thus extremely slow. In fact, the dynamics is so slow that we do not see globule formation with $z = 1$ on the time scales of our simulation.

A very different mechanism emerges when condensation is induced by multivalent cations. As soon as the Manning parameter $\xi_M = l_B/b > 1/z$, some of the ions are condensed. A counterion can locally neutralize the negative charge on the monomer, and the resulting bound species has an effective charge $(z - 1)e$. Bare monomer charges that are separated by a large distance along the contour can be attracted to the positive charge a process referred to as "ion bridging". The range over which such attractive interactions are effective increases with z (see below). Since the size (and hence the number of clusters) of the clusters is controlled by the length of

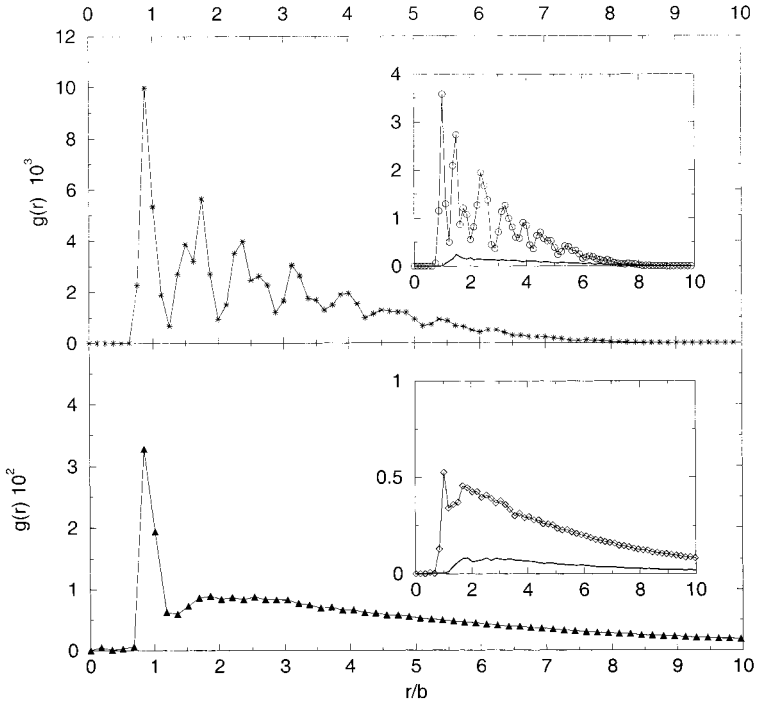

Figure 7. Pair correlation function for the combined system of the PE chain ($N = 240$) and the counterions ($z = 2$) in long time limit ($t \approx 600\tau$). The system is quenched to $l_B = 5.0b$. Top: $v_2 = -0.06b^3$. Bottom: $v_2 = -62.34b^3$. The insets show the correlation functions between monomers (symbols) and counterions (solid lines). The lack of correlations between counterions is evident.

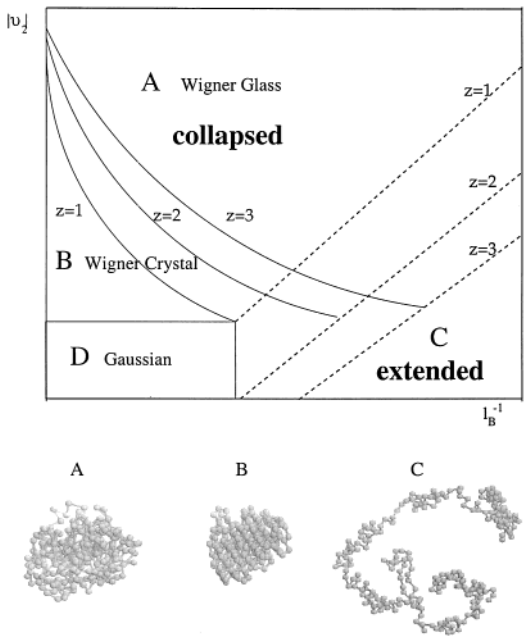

Figure 8. Valence dependent diagram of states in the ($|v_2|$ and l_B^{-1}) plane for strongly charged PE. The dashed lines represent the boundary between between stretched and collapsed states and depend on z. The z-dependent solid lines in the collapsed region separate the Wigner crystal region from the Wigner "glassy" region.

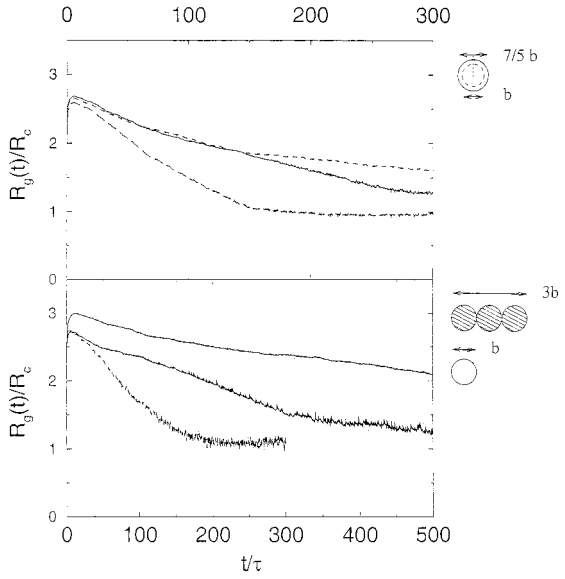

Figure 9. (a) Time dependence of $\langle R_g(t)\rangle$ ($N = 240$) for different sizes of the counterions ($z = 2$) for $v_2 = -3.69b^3$, $l_B = 5.0b$. The top curve (dotted line) is for $R = {}^5/_7$ and the dashed line is for $R = 2$. For comparison, results for the condition $R = 1$ are also displayed as solid line. (b) Plot of $\langle R_g(t)\rangle/R_c$ as a function of t for different shapes and z of counterions. The top curve is for spherical monovalent case, the middle is for connected trivalent counterions, and the bottom curve represents a spherical counterion with $z = 3$. The solvent condition corresponds to $v_2 = -15.2b^3$ ($\epsilon_{LJ} = 1.5$).

the contour over which ionbridges form, it follows that the efficiency of collapse should also increase with z.

An approximate estimate the range of the effective attraction induced by cations with $z \geq 2$ can be made by considering the fluctuation induced potential between like-charged particles in the presence of multivalent cations. Netz and Orland[34] have recently shown that there is a correction to the usual Debye−Hückel potential in electrolytes. The resulting attractive potential depends on the ionic strength of the solution. Their results can be adopted to the PE problem provided we can neglect the loop entropy of the polymer due to ionbridging. The monomers of the PE backbone gives rise to an attractive potential $\Delta U \approx (1 - z^2)cl_B{}^3e^{-\kappa r}/\kappa r$ provided $z \geq 2$. Here $\kappa^2 = 4\pi l_B(z^2 + 1)c$ where c is the concentration of counterions. Because of charge neutrality in our model system there is a finite value for c. With this form of the potential, it is clear that there is a

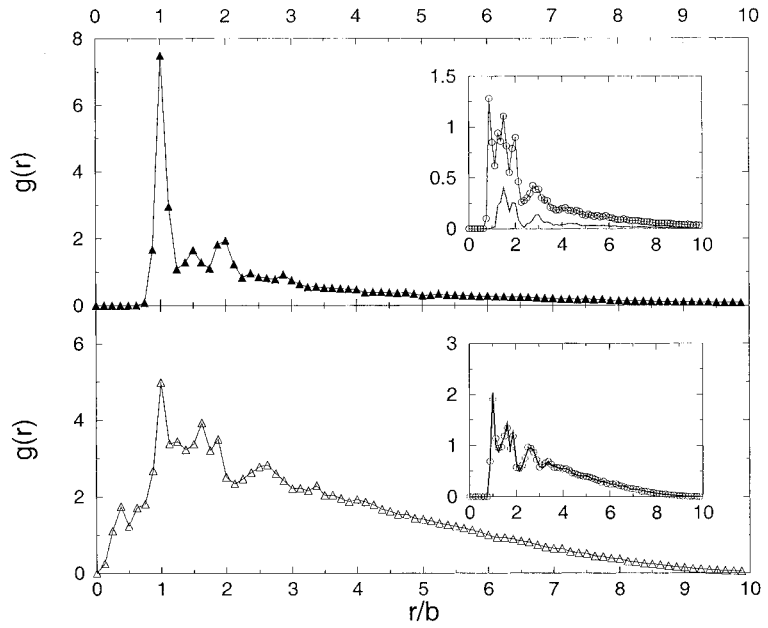

Figure 10. (a) Pair correlation function for spherical counterions whose size is larger than the monomers ($\sigma_c/\sigma_m = {}^7/_5$). (b) Pair correlation function with connected trivalent counterions. Curves in insets show monomer−monomer (shown in circles) and counterion−counterion (solid lines) correlation functions. These two curves are superimposable in part b. The value of v_2 is the same as in Figure 9b.

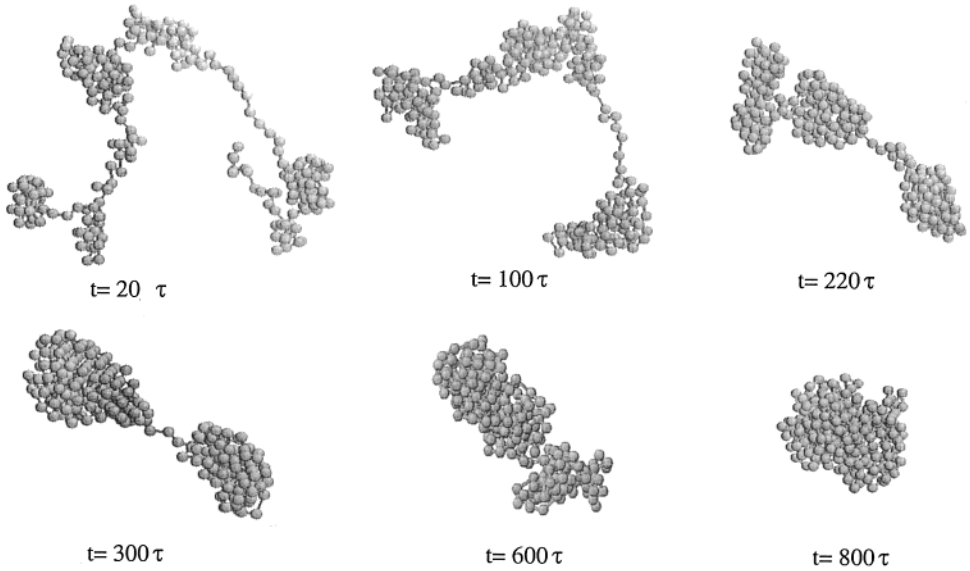

Figure 11. Snapshots as a function of time for homopolymer (neutral chain) collapse with $\epsilon_{LJ} = 2.0$ which corresponds to hydrophobic solvent conditions. The formation of clusters and their subsequent merger at later times is evident.

negative correction to the bare v_2 which decreases as z increases. This implies that the strength of the induced attractions upon condensation of counterions increases with z. The range over with ion bridging occurs can be estimated by balancing ΔU and k_BT and we obtain $r_t \approx (z^2 - 1)l_B{}^{5/2}c^{1/2}/(z^2 + 1)^{1/2}$ in the limit of small c. Because of the increase of r_t with z we expect that the number of initial clusters in the metastable pearl-necklace structures must decrease with z and this leads to more efficient collapse of the PE chain.

The qualitative arguments given above are reflected in our simulations which show that the number of globules in the necklace decreases with increasing z. Thus, higher valence counterions give rise to smaller number of pearls in the intermediate necklace globule by forming "ion-bridging" structure. To probe the mechanism of cluster formation by bridging segments of the chain separated by many monomer units (ion-bridging) due to counterion condensation we have calculated the time dependence of the correlation function

$$c(t) = \sum_{i<j,|i-j|\geq 5} H(2b - |r_i - r_j|) \qquad (6)$$

where $H(x)$ is the Heavyside function. Figure 5 shows $c(t)$ as a function of t for all $z = 1 - 4$ at nearly Θ-solvent conditions ($\epsilon_{LJ} = 0.3$). This figure shows that contacts between monomers that are separated by at least four bonds occur more rapidly as z increases. Within the typical error bars in our simulation we find little difference between $z = 3$ and $z = 4$. This is because, as explained earlier, the condensation mechanism in both cases is similar. This leads to rapid condensation of the chain as the valence of the counterions becomes larger.

The general mechanism that leads to cluster formation occurs as soon as the counterions condense. Since the condensation process is diffusion-limited it follows that the different mechanisms as a function of z must be evident early in the collapse process. To illustrate this we have calculated the probability of loop formation as a function of loop length l for various values of z at a fixed time $t = 10\tau$. The result, displayed in Figure 6 shows that for both mono and divalent cations only small loops are likely to form; i.e., the clusters are "local". However for $z \geq 3$, there is a probability of forming large loops leading to ion-bridging which effectively reduces the number of clusters.

In Figure 4, we show snapshots of compact intermediate pearl necklace structures for $z = 2$ at $\epsilon_{LJ} = 1.5$ ($v_2 = -15.2b^3$). These snapshots are in accord with the general mechanism for multivalent ion condensation induced collapse of the polyelectrolyte chain. For large z the number of cluster formed is small, but the sizes of clusters are bigger at $t \approx \tau_{CLUST}$. Note that the dynamics are faster with larger valence. It should be noted that extended necklace globule structures are predicted to be the equilibrium conformations of weakly charged polyelectrolytes in the absence of Manning condensation in poor solvents.[25,29] Here we find them as metastable intermediates enroute to the globular state.

D. Structure of the Collapsed Globules. For $z \geq 2$ the equilibrium globular conformation is kinetically reached at all negative value of v_2. However, the arrangement of the monomers and counterions in the globular structure depends very critically on the ratio v_2. When $|v_2|$ is large enough but not too large (this is made precise in section E) then the combined system of counterions and the polyelectrolyte forms a Wigner Crystal (top panel of Figure 7). As $|v_2|$ is increased we find that the globular polyelectrolyte and counterions tend to form an amorphous (Wigner glass) like structures (see bottom panel of Figure 7). It is not clear whether these are equilibrium glassy structures. Our simulations indicate that the approach to the ordered structure is extremely slow when $|v_2|$ becomes sufficiently large, i.e., there appears to be manifestations of glassy dynamics.

The differences in the morphology of the structures is best seen in the dynamic structure factor $g(r)$ for relatively good solvents and extremely poor solvents at long times ($t > 350\tau$). From the top panel in Figure 7, which shows a plot of the pair distribution function $g(r)$ for $v_2 = -0.06b^3$, $l_B = 5.0b$, and $z = 2$, we infer that the combined system of counterions and the polyelectrolyte forms a Wigner crystal. The formation of a Wigner crystal is seen by the presence of several peaks in $g(r)$ at long times ($t > 600\tau$). The analysis of the peak positions reveals that the ordered structure corresponds to a bcc lattice. The ordering is considerably fuzzy (see bottom panel of Figure 7) when the solvent quality is extremely poor ($\epsilon_{LJ} = 3.0(v_2 = -62.34b^3)$). The resulting structure is amorphous (Wigner glass). Thus, for $v_2 = -62.34b^3$ the dynamics of approach to the ordered state is slow.

The formation of Wigner crystal (the structure of the combined PE chain and condensed counterions) is superficially similar to the proposed mechanism for attraction between like charged rodlike polyelectrolytes.[2,35] Shklovskii,[36] extending the proposal by Rouzina and Bloomfield,[12] showed that upon condensation of multivalent cations onto a negatively charged rodlike molecules, there develops spatial correlations between the counterions. This leads to the crystallization of the counterions and the cohesive (or binding) energy of the crystals is the source of attraction. For rod molecules this would imply that the radial distribution function (or structure factor) of the *counterions alone* will have peaks at positions reflecting the structure of the underlying lattice. In the case of the collapsed flexible PE we find that the monomers as well as the counterions are arranged in a periodic fashion. Just as in the rod polymers the cohesive energy of the Wigner crystal is the major driving force for globule formation provided the strength of the hydrophobicity is not overwhelming. In the flexible PE collapse case a solid solution (for example $MgCl_2$ for $z = 2$) is a good model for describing the structure of the globule.

When the solvent hydrophobicity is strong we find that the globule is a Wigner or ionic glass. Solis and Olvera de la Cruz[37] have argued that such collapsed structures result because the combined effects of finite size and chain connectivity lead to defects that do not anneal for long times. This suggestion is consistent with our simulations provided the solvent is sufficiently hydrophobic. Even in this situation the cohesive energy of the ionic glass is less than the free energy of the expanded PE chain so that one observes the formation of globules at low temperatures.

E. Phase Diagram in the (v_2, z) Plane. The observations concerning the structure of the collapsed globules together with simple scaling arguments can be used to construct a valence-dependent phase diagram for strongly charged polyelectrolytes in poor solvents (second virial coefficient $v_2 < 0$). When counterion condensation takes place, the decrease in the effective charge of the polyanion can be computed by equating the chemical potential of the free and condensed counterions (two-phase approximation). Generalizing the arguments of Schiessel and Pincus[18] to arbitrary z, we find that the total charge of the polyelectrolyte decreases from Nf ($f = 1$ in our simulation) to $N\bar{f} \approx \kappa L/l_B)(1/z)$ where $\kappa \approx -ln\phi$ and is the volume fraction of the free counterions. The size of the polyelectrolyte is given by $L \approx \kappa^2 b^2 N/l_B z^2$ provided $l_B > \kappa^2 z^{-2} b N^{1/2}$. As the quality of the solvent decreases to a level such that thermal blob size $\xi_T \approx b^4/|v| < \xi_{el} \approx l_B z^2/\kappa^2$ (size of the electrostatic blob) then the chain condenses to a globule. The boundary dividing the stretched and collapsed conformation is obtained by equating ξ_{el} and ξ_T and is given by $|v_2| \approx b^4\kappa^2/l_B z^2$.

In the globular phase, we find two regimes, one corresponding to the Wigner crystal and the other a Wigner glass. The boundary between the two is obtained by equating the gain in the energy upon condensation ($\approx ze^2/d\epsilon$) to the attractive interaction due to the poor solvent quality (kTv^2b^{-6}). This leads to the condition $|v|_{ca} \approx z^{1/2}b^{5/2}l_B^{1/2}$. To determine the boundary more precisely we have to account for the induced attraction between monomers after counterion condensation. Thus, the actual determination of the boundary separating the Wigner crystalline regime and the glassy regime requires equating $ze^2/d\epsilon$ and $kTv_{2R}^2b^{-6}$ where v_{2R} is the renormalized second virial coefficient. This argument again shows that the shape of the PE chain requires, in a nontrivial way, the coupling of electrostatic interactions and effects coming from solvent quality. In light of this, the boundary indicated in Figure 8 should be regarded as qualitative.

The boundary between the two collapsed phases is difficult to determine from the simulation because of the extreme slow dynamics in glassy phase. For the purpose of illustrating the phase diagram, we assume that the ionic glass is an equilibrium phase. To validate the phase diagram, we performed extensive simulations for all z (=1, 2, 3, 4). The structural conformations are in qualitative accord with the predicted phase diagram.

F. Effect of Size and Shape. In the discussions so far, we have assumed that the size of the counterions is the same as the monomer. Oosawa has argued that the fraction of condensed counterions is not significantly changed by altering the size of the counterions provided the volume fraction of the polyanion is small.[38] Since the correlation between the monomers and counterions is dependent on the size of the counterions the dynamics of collapse should be sensitive to $R = \sigma_m/\sigma_c$ where σ_c is the size of the counterions. We carried out simulations for $R = 2$ and $R = {}^5/_7$ with $v_2 = -3.69b^3$ for $N = 240$ at $l_B = 5.3b$. For $R = 2$ we find that the rate of globular formation in enhanced compared to $R = 1$ for $z = 2$, 3, and 4. The difference between the two cases is most dramatic for $z = 2$ (see Figure 9a). For the divalent cation, globular formation occurs at $t \approx 300\tau$ when $R = 1$ (see Figure 9a). However, when the size of counterions is made smaller the PE chain almost reaches the globular state at $t \approx 150\tau$. Conversely, when the size of the counterion is increased the efficiency of collapse decreases (see Figure 9a). This establishes the importance of the size of the counterion, and in particular the correlation between them in determining collapse dynamics.

The inverse correlation between the size of the counterion and the efficiency in inducing collapse (at fixed z) can be qualitatively understood in terms of our proposed collapse mechanism. In our picture the PE chain forms metastable pearl-necklace structures when counterions condense. The dynamics is dictated both by the precise structure of the clusters and by their subsequent merger (Lifshitz−Slyozov mechanism). When the size of the counterions is large, the spatial correlation between the condensed counterions (whose range is approximately $2\sigma_c$) becomes greater than b. This prevents neutralization of all backbone charges on length scales $\approx 2\sigma_c$. As a result, there are potentially several uncompensated charges in the clusters. Such charges can form ion bridging structures especially when $z \geq 2$. These structures would involve pairing between unlike charges that are separated by several σ_c. In all likelihood these structures would be incompatible with the ordered globule. The rapid initial formation of such frustrated globules, when $(2\sigma_c/b > 1)$ slows down the dynamics of the collapse of the chain. For $R = {}^5/_7$ we find that at $t \approx 300\tau$ is nearly twice as large as the compact globule (see Figure 10a). Examination of the conformations suggest that large spatial fluctuations, which are intrinsically slow, are required for transition to the ordered globular state. The correlation function with larger counterions ($R = {}^5/_7$ case) is shown in Figure 10a.

The effects of counterion−counterion correlation in dictating the collapse dynamics also suggests that counterion shape would be a significant factor in PE collapse. It is known that in the collapse of DNA (a stiff chain) $CO(NH_3)_6^{3+}$ (roughly spherical) is a more efficient condensing agent than the isovalent counterion spermidine which is more aptly described as an extended cigarlike object with three centers at which a $+e$ charge is localized. To examine the shape of the counterion on the collapse of flexible PE chains, we considered a trivalent counterion composed of three monovalent counterions connected by two springs. The spring constant is taken to be $10k_BT/b^2$. The equilibrium distance between two successive positive charges is b. Because of the connectivity, we expect the mobility to be reduced compared to the isovalent but spherical counterions. This is reflected in the condensation rate, which is found to be smaller for the elongated counterion.

The effect of shape on the collapse dynamics was examined in hydrophobic solvent ($\epsilon_{LJ} = 1.5$, $v_2 = -15.2b^3$). Under this solvent condition, there is a coil to globule transition even with monovalent counterions. However, the dynamics is slow so that we could not observe the complete transition to the globular conformation even at $t \approx 500\tau$ (Figure 9b). For the connected trivalent counterions, we expect significantly larger spatial correlation between the condensed counterions than for the spherical isovalent counterion. According to the arguments given above we would expect that the collapse dynamics is slower for the connected trivalent counterion than for the spherical counterpart. This expectation is borne out in our simulations (see Figure 9b). The difference in efficiency between trivalent counterions and monovalent ions can be explained in terms of the difference in z. The structure of the globule formed in the presence of the connected trivalent counterion is ordered. The pair correlation function for the combined PE chain and for the monomers and counterions are shown in Figure 10b. There are well-defined peaks whose positions correspond to that expected for a bcc microcrystallite. Surprisingly, we find that, in contrast to the situation in Figure 7, the monomers and counterions are also ordered. The cohesive energy upon globule formation is the driving force toward globularity.

4. Comparison with Kinetics of Homopolymer Collapse

Although no complete theory exists for describing all the features of the better studied problem of the dynamics of homopolymer collapse, a general scenario for globule formation in these systems has emerged. Beginning with the work of de Gennes,[16] it has been known that upon a quench to $T < \Theta$ local clusters form at early times. The clusters are composed of monomers that are relatively close along the contour of the chain. At longer times, there is a coarsening of the locally formed clusters until the globule is reached.

The outlines of the collapse of homopolymers appear to be similar to the general mechanism for the kinetics of PE collapse that we have described in this article. To make a direct comparison we also simulated, by integrating Langevin equations, homopolymer collapse with $N = 240$ with $\epsilon_{LJ} = 2.0$. This corresponds to neutral chain in a hydrophobic solvent ($v_2 = -25.8b^3$). A series of snapshots in Figure 11 shows the expected picture of the collapse process. Initially a number of local clusters form and over time these clusters merge to form the compact globule. Qualitatively this coarsening is like the Lifshitz−Slyozov process. However, it has been suggested that the exponents characterizing the growth of the clusters are different from that found for PE and polyampholyte collapse.

Despite the overall similarity[39] in the collapse mechanism between PE and homopolymers there are some

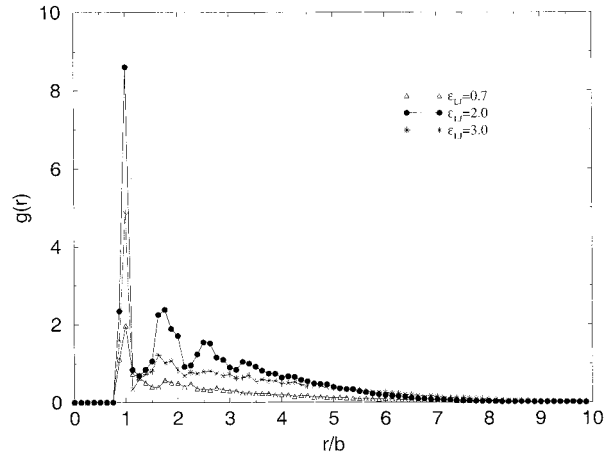

Figure 12. Pair correlation function for homopolymer for three values of ϵ_{LJ} indicated in the figure. The values of ϵ_{LJ} span the range of solvent conditions. The fuzzy nature of the peaks indicates lack of order in the structures.

fundamental differences. (a) The internal structure of the globular state for homopolymers is fluidlike with short range order. This is most vividly seen in Figure 12 which shows the monomer−monomer distribution function for homopolymers in three poor solvent conditions. The peaks are relatively dispersed. The distribution function for the most ordered globule ($\epsilon_{LJ} = 2.0$) is similar to that seen in dense Lennard-Jones fluid. In contrast the collapsed PE chain along with counterions is ordered in the Wigner crystalline state. Such ordering is already evident in the intermediate stages in which clusters form. Even under conditions in which ionic glass forms it is evident that there is considerable order in the collapsed structures compared to the homopolymer. (b) The rate of coarsening of clusters is smaller in homopolymers than in PE chains because the number of initial clusters in the latter case is relatively large. Because the range of attraction (the strength is $\approx k_B\Theta$) between the thermal blobs (size $\xi_T \approx b^4/v_2$) is short many local clusters form following a quench. The "nucleation" of the large number of clusters accounts for the slow dynamics. The reduction in the number of clusters is achieved in PE by altering a number of factors such as z, l_B, v_2, and the shape of the counterions. (c) Perhaps the most significant difference between the two cases is that in PE counterions play a profound role in controlling the collapse kinetics. It is crucial to include spatial correlation between counterions to describe both the structural and dynamical properties of PE in poor solvents. Thus, the physical processes involved in the generation of the metastable pearl-necklace structures is very different in PE than in homopolymers.

5. Conclusions

The findings presented here show that a bewildering range of dynamical behavior is to be expected in the collapse of strongly charged polyelectrolytes mediated by counterion condensation. The prediction that the formation of ordered states Wigner crystal and amorphous structure (Wigner glasses) should depend on the quality of the solvent should be amenable to experimental (neutron or light scattering) tests. Even if the Wigner glass is metastable our simulation suggest that the dynamics in the two regions (see Figure 8) covering the globular states of PE should be dramatically different and depend on the valence of the counterions. Our analysis also suggests that a theory describing collapse dynamics in polyelectrolytes must take into account the microscopic correlations between the counterions and the PE density fluctuation describing the globular structure. Thus, it is unlikely that a single parameter such as an effective persistence length (even if it is made to be dependent on scale) for PE can adequately represent the kinetics of the collapse process.

Acknowledgment. We thank M. Olvera de la Cruz, B.Shklovskii, and Y. Levin for useful discussions. This work was supported by a grant from the National Science Foundation (NSF CHE 99-75150).

References and Notes

(1) Bloomfield, V. A. *Biopolymers* **1991**, *31*, 1471; *Curr. Opin. Struct. Biol.* **1996**, *6*, 334.
(2) For attractive interactions between like charged rods induced by correlations in counterions, see: Ha, B.-Y.; Liu, A. J. *Phys. Rev. Lett.* **1997**, *79*, 1289; **1998**, *81*, 1011.
(3) Gønbech-Jensen, N.; Mashl, R. J.; Bruinsma, R. F.; Gelbart, W. M. *Phys. Rev. Lett.* **1997**, *78* 2477.
(4) Podgornik, R.; Parsegian, V. A. *Phys. Rev. Lett.* **1998**, *80*, 1560.
(5) Gosule, L. C.; Schellman, J. A. *Nature* **1976**, *259*, 333. Gosule, L. C.; Schellman, J. A. *J. Mol. Biol.* **1978**, *121*, 311. Chattoraj, D. K.; Gosule, L. C.; Schellman, J. A. *J. Mol. Biol.* **1978**, *121*, 327.
(6) Widom, J.; Baldwin, R. L. *J. Mol. Biol.* **1980**, *144*, 431.
(7) Delsanti, M.; Dalbiez, J. P.; Spalla, O.; Belloni, L.; Drifford, M. *ACS Symp. Ser.* **1994**, *548*, 381.
(8) Gonzalez-Mozuelos, P.; Olvera de la Cruz, M. *J. Chem. Phys.* **1995**, *103*, 3145.
(9) Olvera de la Cruz, M.; Belloni, L.; Delsanti, M.; Dalbiez, J. P.; Spalla, O.; Drifford, M. *J. Chem. Phys.* **1995**, *103*, 5781.
(10) Odijk, T. *J. Polym. Sci.* **1977**, *15*, 477.
(11) Skolnick, J.; Fixman, M. *Macromolecules* **1977**, *10*, 944.
(12) Rouzina, I.; Bloomfield, V. A. *J. Phys. Chem.* **1996**, *100*, 4292, 9977.
(13) Stevens, M. J.; Kremer, K. *J. Chem. Phys.* **1995**, *103*, 1669.
(14) Micka, U.; Holm, C.; Kremer, K. *Langmuir* **1999**, *12*, 4033. Micka, U.; Kremer, K. *Europhys. Lett.* **2000**, *49*, 189.
(15) Winkler, R. G.; Gold, M.; Reineker, P. *Phys. Rev. Lett.* **1998**, *80*, 3731.
(16) de Gennes, P. G.; Pincus, P.; Velasco, R. M.; Brochard, F. *J. Phys. (Paris)* **1976**, *37*, 1461.
(17) Barrat, J.-L.; Joanny, J.-F. *Adv. Chem. Phys.* **1996**, *XCIV*, 1.
(18) Schiessel, H.; Pincus, P. *Macromolecules* **1998**, *31*, 7953.
(19) Khokhlov, A. R.; Kramarenko, E. Y. *Macromolecules* **1996**, *29*, 681.
(20) Klooster, N. Th. M.; van der Touw, F.; Mandel, M. *Macromolecules* **1984**, *17*, 2070.
(21) Starodoubtsev, S. G.; Khokhlov, A. R.; Sokolov, E. L.; Chu, B. *Macromolecules* **1995**, *28*, 3930.
(22) Brilliantov, N. V.; Kuznetsov, D. V.; Klein, R. *Phys. Rev. Lett.* **1998**, *81*, 1433.
(23) Manning, G. S *J. Chem. Phys.* **1969**, *51*, 924.
(24) Khokhlov, A. R. *J. Phys. A* **1980**, *13*, 979.
(25) Dobrynin, A. V.; Rubinstein, M.; Obukhov, S. P. *Macromolecules* **1996**, *9*, 2974.
(26) Lyulin, A. V.; Duenweg, B.; Borisov, O. V.; Darimskii, A. A. *Macromolecules* **1999**, *32*, 3264.
(27) Lord Rayleigh. *Philos. Mag.* **1882**, *14*, 184.
(28) Solis, J. F.; Olvera de la Cruz, M. *Macromolecules* **1998**, *31*, 5502.
(29) Kantor, Y.; Kardar, M. *Europhys. Lett.* **1994**, *27*, 643.
(30) Allen, M. P.; Tildesley, D. J. *Computer Simulation of Liquids*; Clarendon Press: Oxford, England, 1990.
(31) Pitard, E.; Orland, H. *Europhys. Lett.* **1998**, *41*, 467. Pitard, E.; *Eur. Phys. J. B* **1999**, *7*, 665.
(32) Lifshitz, I. M.; Slyozov, V. V. *J. Phys. Chem., Solids* **1961**, *19*, 35.
(33) Lee, N.; Thirumalai, D. *J. Chem. Phys.* **2000**, *113*, 5126.
(34) Netz, R. R.; Orland, H. *Europhys. Lett.* **1999**, *45*, 726.
(35) Levin, Y.; Arenzon, J. J.; Stilck, J. F. *Phys. Rev. Lett.* **1999**, *83*, 2680; *Physica A* **2000**, *283*, 1.
(36) Shklovskii, B. *Phys. Rev. Lett.* **1999**,*82*, 3268.
(37) Solis, F. J.; Olvera de la Cruz, M. *J. Chem. Phys.*, in press.
(38) Oosawa, F. *Polyelectrolytes*; Dekker: New York, 1971.

(39) There is some similarity between the collapse of PE chains and homopolymers. Kuznetsov, Y. A.; Timoshenco, E. G.; Dawson, K. A. *J. Chem. Phys.* **1995**,*103*, 4807. Byrne, A.; Kiernan, P.; Green, D.; Dawson, K. A. *J. Chem. Phys.*,**1995**, *102*, 573. Crooks, G. E.; Ostrovsky, B.; Bar-Yam, Y. cond-mat (9905393)). In contrast to homopolymers, the cluster size formation and their range of interaction is controlled by valence and size of counterions. The dynamics of collapse in PE cannot be described without accounting for correlations between monomers and counterions.

MA001604Q